Mechanism of Tetraalkylammonium Headgroup Degradation in Alkaline Fuel Cell Membranes

ARTICLE *in* THE JOURNAL OF PHYSICAL CHEMISTRY C · FEBRUARY 2008

Impact Factor: 4.77 · DOI: 10.1021/jp7115577

7 AUTHORS, INCLUDING:

Brian R Einsla
Dow Chemical Company
12 PUBLICATIONS **1,522** CITATIONS
SEE PROFILE

Lawrence R. Pratt
Tulane University
203 PUBLICATIONS **8,947** CITATIONS
SEE PROFILE

James M Boncella
Los Alamos National Laboratory
139 PUBLICATIONS **5,097** CITATIONS
SEE PROFILE

Jonathan A. Rau
Los Alamos National Laboratory
4 PUBLICATIONS **174** CITATIONS
SEE PROFILE

THE JOURNAL OF PHYSICAL CHEMISTRY C LETTERS

2008, *112,* 3179−3182
Published on Web 02/09/2008

Mechanism of Tetraalkylammonium Headgroup Degradation in Alkaline Fuel Cell Membranes

Shaji Chempath,[†] Brian R. Einsla,[‡] Lawrence R. Pratt,*[,†] Clay S. Macomber,[‡] James M. Boncella,[‡] Jonathan A. Rau,[‡] and Bryan S. Pivovar[‡]

Theoretical Division, Materials Physics and Applications Division, Los Alamos National Laboratory, Los Alamos, New Mexico 87545

Received: December 7, 2007; In Final Form: January 25, 2008

Cationic headgroups such as tetramethylammonium (TMA) undergo degradation in alkaline conditions through two different mechanisms. In the first mechanism, a hydroxide ion performs an S_N2 attack on the methyl groups and directly forms methanol. In the second mechanism, an ylide (trimethylammonium methylide) and a water molecule are formed by the abstraction of a proton from a methyl group. The ylide subsequently reacts with water to form methanol. Both pathways have the same overall barrier as observed in our reaction path calculations with density functional theory. The ylide mechanism is verified by H−D exchange observed between the aqueous phase and the cationic head group. We also discuss the effect of the medium and the water content on the calculated reaction barriers. Good solvation of the head-groups and hydroxide ions is essential for the overall chemical stability of alkaline membranes.

Introduction

Alkaline membrane fuel cells (AMFC) have the potential to replace the acidic proton-exchange membrane fuels cells (PEMFC) for use in vehicular and portable applications.[1] Alkaline medium allows for the use of nonprecious electrode catalysts made from inexpensive metals such as Fe/Co/Ni and thus avoids the use of rare precious metals such as Pt and Ru.[2] Challenges in the development of AMFCs include the development of stable anion exchange membranes (AEM) at high pH. Polymeric materials such as Nafion, which is a fluorocarbon polymer with side chains ending in sulfonic acid head groups, are used in traditional (acidic) fuel cells. In AEMs, tetraalkylammonium head groups such as $[N(CH_3)_4]^+$ can be employed.[3] Unfortunately, hydroxide ions tend to react chemically with these headgroups.[4] For example, $[N(CH_3)_4]^+$ $[OH]^-$ can undergo an irreversible reaction to give trimethylamine and methanol. The irreversible formation of such neutral species leads to the loss of ionic conductivity and functionality of the membrane. This reaction between cation and hydroxide serves as the ultimate limit for membrane lifetime, and limits the applications where this technology can be applied. In this letter, we report the reaction mechanism of tetramethylammonium-based headgroups, as obtained from density functional theory (DFT) calculations. The importance of the solvation of cations and hydroxide and the effect of solvation on membrane stability will also be discussed. Experimental verification of reaction products in support of the reaction mechanism is also presented.

* Author to Whom Correspondence should be Addressed. Phone: 505-667-8624. Fax: 505-665-3909. E-mail: lpratt@tulane.edu.
[†] Theoretical Division.
[‡] Materials Physics and Applications Division.

Methods

B3LYP DFT and 6-311++g(2d,p) basis set as implemented in *Gaussian 03*[5] software is used for obtaining the optimized geometries of all species. A polarizable continuum model (PCM) as implemented in *Gaussian 03* software was used to account for the water medium surrounding the reactive species. We will use the symbol E to refer to the sum of electronic energy and solvation free energy, and the symbol G^0 to refer to the free energy obtained after including vibrational, translational, and rotational degrees of freedom at 298 K. A growing string algorithm was used to find the reaction path connecting the reactants and products.[6,7] The highest point on the reaction path is taken as the first approximation for a transition state. The exact transition state (saddle point on the potential energy surface (PES)) is obtained from the approximate transition state by using the Berny optimization algorithm as implemented in *Gaussian 03* software. Descriptions of the thermogravimetry (TG) and mass spectroscopy (MS) experiments and degradation experiments are presented along with the results in the next section.

Results and Discussion

Degradation of Tetramethylammonium. $[N(CH_3)_4]^+$ is used as a model cation in our chemical stability studies. In practice, this headgroup is tethered to the polymer backbone through linkages such as $-Ar-CH_2-N(CH_3)_3^+$, where Ar is an aromatic group. Gas-phase optimization of $[N(CH_3)_4]^+[OH]^-$ showed that OH^- prefers to stay in the cleft formed between three methyl groups. However, optimizations with different starting geometries also lead to configurations in which OH^- combines with either a methyl group or a hydrogen (of $-CH_3$) to form methanol or water. Motivated by these gas-phase observations,

10.1021/jp7115577 CCC: $40.75

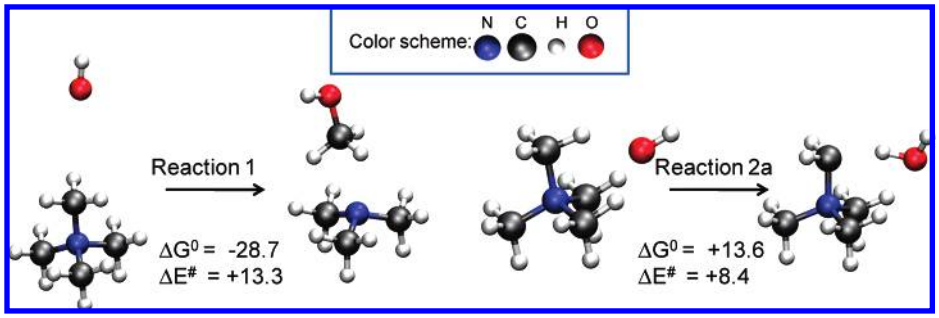

Figure 1. In Reaction 1, OH^- approaches from above the methyl group and leads to the formation of methanol. In Reaction 2a, OH^- approaches close to the hydrogens of the methyl and extracts a $-CH_3$ proton. These geometries are obtained by optimization with PCM solvation, and energies are in kcal/mol.

we studied the reaction of OH^- and $[N(CH_3)_4]^+$ in aqueous phase with a PCM, setting the dielectric constant of water, ϵ, to be 78.39. The free energy changes and activation energy barriers (in kcal/mol) are given below. The reactant and product structures are also depicted in Figure 1.

$$[N(CH_3)_4]^+ + OH^- \rightarrow N(CH_3)_3 + CH_3OH$$
$$\Delta G^0 = -28.7; \qquad \Delta E^{\#} = +13.3 \quad (1)$$

$$[N(CH_3)_4]^+ + OH^- \rightarrow CH_2{=}N(CH_3)_3 + H_2O$$
$$\Delta G^0 = +13.6; \qquad \Delta E^{\#} = +8.4 \quad (2a)$$

$$CH_2{=}N(CH_3)_3 + H_2O \rightarrow N(CH_3)_3 + CH_3OH$$
$$\Delta G^0 = -42.3; \qquad \Delta E^{\#} = +5.3 \quad (2b)$$

All energies are reported with respect to the reference state in which reactants are solvated separately in water. Note that the $\Delta E^{\#} = 5.3$ kcal/mol for reaction 2b is reported with respect to the reactants for that elementary reaction, which is the stable ylide intermediate shown on the right-hand side of reaction 2a in Figure 1. Note that the formation of methanol is thermodynamically favorable by −28.7 kcal/mol, and these degradation reactions are practically irreversible. The activation energy barrier $\Delta E^{\#}$ for the S_N2 reaction is only 13.3 kcal/mol ($\Delta G^{0,\#}$ after including the vibrational, rotational, and translation degrees of freedom and changing the standard state to 1 mol/L is 20.7 kcal/mol), and the application of absolute rate theory gives a rate constant of 0.01 L/mol/s at 298 K (0.33 L/mol/s at 353 K). Such estimates are very approximate because the chemical interaction of OH^- with the surrounding water molecules is only implicitly taken into account in the PCM model. There are also errors associated with the energies evaluated with DFT. For example, the energy of formation with B3LYP/6-311++g(2d,p) level theory is expected to have an average error of 3.1 kcal/mol based on comparison of theory and experiment in case of the G2 molecule set.[8] We use the calculated activation barriers as a qualitative tool to compare different reaction mechanisms, and a quantitative agreement with experiments is improbable. To check the effect of the level of theory used, we reevaluated the S_N2 activation barrier with geometries obtained at MP2/6-311++g(2d,p) level theory and found that the activation barrier increased by 5 kcal/mol (18.3 instead of 13.3 kcal/mol).

The small barrier (8.4 kcal/mol) calculated for ylide formation (Reaction 2a) suggests that an equilibrium between starting materials and ylide should occur if this mechanism is involved in $N(CH_3)_3$ formation when tetramethylammonium hydroxide decomposes. Thus, the rapid scrambling of methyl protons and aqueous protons should be observable in H−D isotope exchange experiments. Mass spectrometry of the gases released in the thermal decomposition of $[N(CH_3)_4]^+[OD]^-\cdot 5(D_2O)$ does indeed

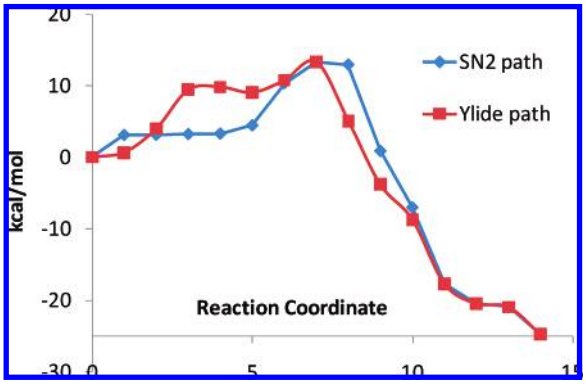

Figure 2. Variation of energy E, as obtained with PCM solvation model along S_N2 and ylide reaction paths. Each point on the graph refers to an intermediate configuration on the minimum energy path that connects the reactant configuration to the product configuration.

reveal rapid scrambling of the protons of $[N(CH_3)_4]^+$ with the $[OD]^-$ and D_2O. TG−MS experiments were performed with a Mettler-Toledo 851 TG coupled to a Pfeiffer Thermo-Star MS for isotopic analysis. The system was configured as an open flow reactor with a nitrogen gas purge. Solid $[N(CH_3)_4]^+[OD]^-\cdot 5(D_2O)]$ was held isothermally at 170 °C, and the evolved gases from the decomposition were carried along a heated transfer line to the MS. In the absence of the ylide mechanism, the main product should be $N(CH_3)_3$ with a molecular mass of 59, whereas the mass spectrum of the $N(CH_3)_3$ produced upon thermolysis reveals the presence of species with higher molecular masses up to 65, thus verifying H−D exchange.[9,10] These results demonstrate that the ylide mechanism plays a crucial role in the decomposition of tetramethylammonium hydroxide. The formation of ylide intermediates is also consistent with results of earlier pyrolysis experiments on tetramethylammonium hydroxide.[11,12]

The overall energy profiles for S_N2 and ylide formation pathways are depicted in Figure 2. Coordinates of the intermediate structures are available in the Supporting Information. The ylide reaction path contains two sections (Reactions 2a and 2b) and thus consists of two potential energy maxima and one intermediate minimum as shown in Figure 2. It should be noted that the second part (Reaction 2b) of the ylide pathway goes through the same transition state structure as the S_N2 path. Because the overall barrier is the same in both pathways, we need to consider only the S_N2 reaction barrier in comparing different reactants for their overall stability. However, additional reactions that are not considered here may occur starting from the ylide intermediate. For example, an aromatic tether may undergo rearrangement reactions with the $N{=}CH_2$ group of the ylide intermediate. Thus, it is important to consider the formation

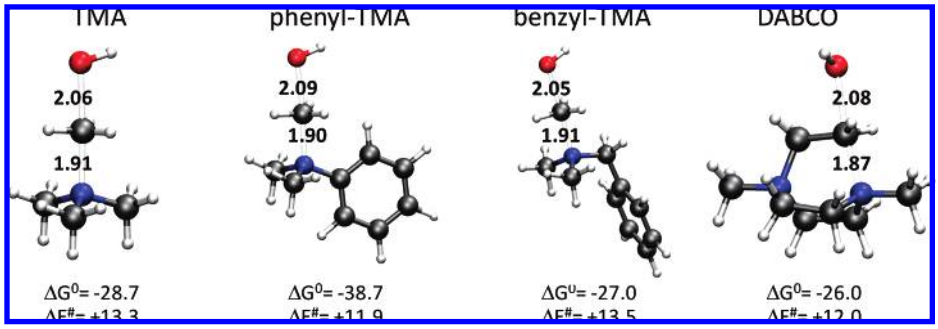

Figure 3. Transition state structures for the S_N2 attack on tetramethylammonium (TMA), phenyltrimethylammonium (phenyl-TMA), benzyltrimethylammonium (benzyl-TMA), and diazabicyclooctane (DABCO). These saddle-point geometries were obtained with B3LYP/6-311++g(2d,p) level theory and PCM solvation model. Free energy changes (i.e., ΔG^0 between reactants and products) and activation energy barriers ($\Delta E^{\#}$) are reported in kcal/mol. The distances of the planar CH_3 moiety to O and N atoms are displayed in Å.

of ylides in examining the stability of tethered tetraalkylammonium headgroups.

Degradation of Modified Cations. Tethering of the tetramethylammonium headgroup to the backbone of the polymer chains can be done through a benzyl or phenyl type of attachment. Groups such as 1,4-diazabicyclo[2.2.2]octane (DABCO) can be used to form cross-linked polymers in which the DABCO group acts as a dicationic crosslinker.[13] In Figure 3, the transition state structures for the degradation of these modified cations via the S_N2 mechanism and the corresponding activation barriers are given. Note that these transition state structures have very similar geometries and have activation barriers in the range of 12−14 kcal/mol. Our overall assessment within the errors associated with DFT is that the addition of phenyl and benzyl groups to the tetramethylammonium does not seem to affect cation stability in a significant way. However, a better assessment can be obtained with direct experimental observation of degradation as given below.

Degradation studies were conducted in sealed Teflon tubes and concentration of cations was observed as a function of time.[9,14] It was found that 90% of benzyl-TMA remained in basic solutions kept at 80 °C after 29 days. Under the same conditions, phenyl-TMA degraded much faster and only 30% of the cations remained in solution. Accelerated degradation studies were done at higher temperature and a range of concentrations in water. In general, the cations degraded much faster at higher concentrations in water, and once again benzyl-TMA proved more stable than phenyl-TMA. For example, at 10 wt % solution of cation in water less than 10% of phenyl-TMA remained after 8 h at 120 °C while more than 80% of benzyl-TMA was left behind.

Effect of Dielectric Medium. In an alkaline membrane operating under fuel cell conditions, a significant fraction of the membrane is occupied by the nonaqueous phase (for example, the polymer backbone) with the balance as the aqueous phase (water, cationic headgroups, and OH^-). When water is removed from the membrane through drying, less water is available for solvation of the ions. In the absence of water, OH^- ions and the cations are not solvated and can become much more reactive. To probe the effect of water and solvation on reactivity, we repeated the ΔG^0 and $\Delta E^{\#}$ evaluations with different dielectric constants in the PCM model, ranging from $\epsilon = 80$ down to $\epsilon = 2$. The geometries of reactants, transition state, and products were kept fixed, and only the dielectric constant was varied among these calculations. Re-optimization of geometries only changed the results within 0.2 kcal/mol. Both the reaction barrier and the free energy change decreases with decreasing dielectric constant as shown in Figure 4. This is because at lower dielectric constants the OH^- on the reactant

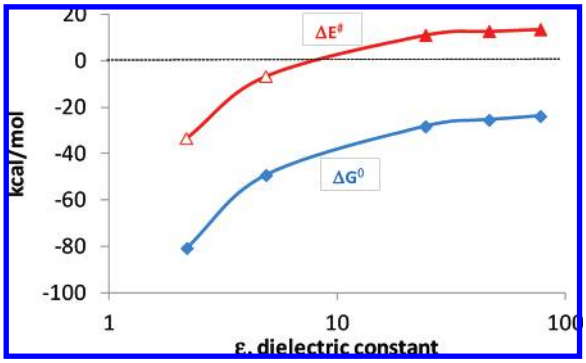

Figure 4. Change in standard free energy (ΔG^0) and activation energy barrier ($\Delta E^{\#}$) for the degradation of tetramethylammonium as a function of the dielectric constant used in the PCM model. Note that a $\Delta E^{\#}$ value below zero (open red triangles) indicates a reaction without activation barriers and thus limited only by diffusion.

side is not solvated well. Note that at dielectric constants below 10, the activation barrier $\Delta E^{\#}$ disappears and the reaction becomes instantaneous (diffusion limited). At a dielectric constant of 5, there exists a transition state structure corresponding to the umbrella inversion of the CH_3 group. However, such a structure is lower in energy compared to the total energy of the reactants, $[N(CH_3)_4]^+$ and OH^-, two oppositely charged species positioned far from each other.

Implications for the Design of Cationic Head Groups. Our results indicate that tetraalkylammonium-based cations show reasonable stability in alkaline media. The chemical stability does not change dramatically with the modification of the alkyl group. The solvation of OH^- anions is very important for the stability of the headgroups. Membrane conditions that lead to poor solvation will lead to faster degradation of the cations. In our future work, we will investigate the chemical stability of cationic headgroups and tethers with explicit water molecules and detailed solvation. We are also investigating the morphology of the membrane using molecular dynamics simulations to get a better picture of the solvation of ions within a membrane. A detailed analysis of these results will be published in the future.

Acknowledgment. This work was carried out under the auspices of the National Nuclear Security Administration of the U.S. Department of Energy at Los Alamos National Laboratory under Contract No. DE-AC52-06N A25396. This project was funded by the Office of Basic Energy Sciences under the U.S. Department of Energy.

Supporting Information Available: Cartesian coordinates of reactants, transition states, and products are attached in xyz

format. The reaction path configurations are also included. This material is available free of charge via the Internet at http://pubs.acs.org

References and Notes

(1) Varcoe, J. R.; Slade, R. C. T. *Fuel Cells* **2005**, *5*, 187.

(2) Spendelow, J. S.; Wieckowski, A. *Phys. Chem. Chem. Phys.* **2007**, *9*, 2654.

(3) Hatch, M. J.; Lloyd, W. D. *J. Appl. Polym. Sci.* **1964**, *8*, 1659.

(4) Tomoi, M.; Yamaguchi, K.; Ando, R.; Kantake, Y.; Aosaki, Y.; Kubota, H. *J. Appl. Polym. Sci.* **1997**, *64*, 1161.

(5) Frisch, M. J. T., G. W.; Schlegel, H. B.; Scuseria, G. E.; Robb, M. A.; Cheeseman, J. R.; Montgomery, J. A., Jr.; Vreven, T.; Kudin, K. N.; Burant, J. C.; Millam, J. M.; Iyengar, S. S.; Tomasi, J.; Barone, V.; Mennucci, B.; Cossi, M.; Scalmani, G.; Rega, N.; Petersson, G. A.; Nakatsuji, H.; Hada, M.; Ehara, M.; Toyota, K.; Fukuda, R.; Hasegawa, J.; Ishida, M.; Nakajima, T.; Honda, Y.; Kitao, O.; Nakai, H.; Klene, M.; Li, X.; Knox, J. E.; Hratchian, H. P.; Cross, J. B.; Bakken, V.; Adamo, C.; Jaramillo, J.; Gomperts, R.; Stratmann, R. E.; Yazyev, O.; Austin, A. J.; Cammi, R.; Pomelli, C.; Ochterski, J. W.; Ayala, P. Y.; Morokuma, K.; Voth, G. A.; Salvador, P.; Dannenberg, J. J.; Zakrzewski, V. G.; Dapprich, S.; Daniels, A. D.; Strain, M. C.; Farkas, O.; Malick, D. K.; Rabuck, A. D.; Raghavachari, K.; Foresman, J. B.; Ortiz, J. V.; Cui, Q.; Baboul, A. G.; Clifford, S.; Cioslowski, J.; Stefanov, B. B.; Liu, G.; Liashenko, A.; Piskorz, P.; Komaromi, I.; Martin, R. L.; Fox, D. J.; Keith, T.; Al-Laham, M. A.; Peng, C. Y.; Nanayakkara, A.; Challacombe, M.; Gill, P. M. W.; Johnson, B.; Chen, W.; Wong, M. W.; Gonzalez, C.; Pople, J. A. *Gaussian 03*, Revision C.02; Gaussian, Inc.: Wallingford, CT, 2004.

(6) Chempath, S. C++ source code for implementing the growing string method and finding transition states (http://zeolites.cqe.northwestern.edu/shaji/growstring.html).

(7) Peters, B.; Heyden, A.; Bell, A. T.; Chakraborty, A. *J. Chem. Phys.* **2004**, *120*, 7877.

(8) Foresman, J. B.; Frisch, A. *Exploring Chemistry With Electronic Structure Methods*; Gaussian, Inc.: Pittsburgh, PA, 1996.

(9) Einsla, B. R.; Chempath, S.; Pratt, L.; Boncella, J.; Rau, J.; Macomber, C.; Pivovar, B. *Electrochem. Soc. Trans.* **2007**, *11*, 1173.

(10) Macomber, C. S.; Boncella, J. M.; Janicke, M.; Pivovar, B. S.; Rau, J. A. *J. Therm. Anal. Calorim.*, sumitted for publication, 2007.

(11) Musker, W. K. *J. Am. Chem. Soc.* **1964**, *86*, 960.

(12) Musker, W. K. *J. Chem. Educ.* **1968**, *45*, 200.

(13) Pandey, A. K.; Goswami, A.; Sen, D.; Mazumder, S.; Childs, R. F. *J. Membr. Sci.* **2003**, *217*, 117.

(14) Einsla, B. R.; Chempath, S.; Pratt, L.; Boncella, J.; Pivovar, B. *Electrochem. Soc. Meeting Abstracts* **2007**, *702*, 538.